MULTIPOLAR ELASTIC REPRESENTATION OF DEFECT FIELDS IN METALS-

D. Seif (University of California, Los Angeles), N.M. Ghoniem (University of California, Los Angeles)

OBJECTIVE:

The objective of this study is to develop a hybrid atomistic-continuum method to obtain an elastic representation of radiation-induced defects in α-Fe. This will make available calculations of elastic interaction energies between defects in various strain environments within the framework of continuum elasticity theory.

SUMMARY

In this study, a hybrid method has been developed to couple the results of molecular statics calculations with classical isotropic elasticity theory to extract a continuum representation of various defects through the use of force multipoles. These calculations have provided a means to account for the changes in defect energetics due to local strain environment effects. In uniform strain environments, the use of the elastic dipole tensor is sufficient to calculate the interaction energy. However we find the use of higher order multipole tensors necessary to represent many defects and their interactions in environments with strain gradients, such as the vicinity of grain boundaries or other extended defects. In addition, isotropic elastic Green's functions are found to provide material response very consistent with atomistic simulations when these higher order terms are implemented. We have made calculations of interactions between defects including Fe and He point defects, Fe self-interstitial clusters, He-vacancy clusters, and extended defects in α-iron.

PROGRESS AND STATUS

Introduction

Internal structural components which operate in the nuclear fusion environment are subject to significant damage doses stemming from the onslaught of 14 MeV neutrons produced in the D-T cycle. The internal production of point defects such as self-interstitial atoms (SIA) and vacancies from elastic interactions, and helium from (n,α)-reactions lead to severe material degradation over time, including swelling [1] and low-temperature embrittlement [2]. The prediction of damage evolution and component lifetime is highly dependent upon accurate models of point defect production and interactions within the material. The development of truly predictive long-timescale simulation techniques has been quite scarce in recent history due to the trade-offs between computational efficiency and rigorous physical treatments. While an accurate physical model of damage accumulation and evolution requires a comprehensive understanding of point defect energetics and interactions, there has been an absence in many studies [3,4,5], of the consideration of local strain environment effects on defect migration properties and stability. The goal of this work is to combine atomistic simulation with elasticity theory to implement the method of force multipoles to represent defects, and use continuum elasticity calculations to quantify interactions between these defects and with various strain fields. These interactions can be made available to future KMC simulations to account for strain-biased diffusion, and give a physically-based description of the accumulation and evolution of damage in irradiated metals.

Force Multipole Representation of Defects

The insertion of a point defect into a perfect crystalline lattice creates a displacement field around the defect on surrounding atoms. This displacement field is typically modeled using one of multiple approaches. Eshelby [9] developed a very simple and elegant way to approach the problem within the confines of elasticity theory. He treated the point defect as a center of dilatation, modeled as a spherical inclusion within an elastic isotropic medium, whose strength may be determined from experiment. This model is only suited, however, to describe defects of high symmetry acting in materials with very low anisotropy. Another method, proposed by Kanzaki [6], involves representing the defect as an array of

forces located on neighboring atoms. Generally called the method of 'Kanzaki forces', this method has been successfully implemented in the past, for example, to give the atomic displacements around vacancies in Cu and Al [7]. However, this approach suffers from a few inherent limitations. Among them, the formulation requires the spatial extent of these forces to be as restricted as possible, typically to first nearest neighbor atoms. For this reason, the elastic response of the material must be modeled with complex 'lattice' Green's functions that have no closed form expression [8], to account for the complex displacements inherent in a defected crystalline lattice. In addition, each point force will introduce a singularity, and additional effort will be required in the computations.

For our application, we have found the method of 'force-multipoles' to be most beneficial. In this method, the defect is represented as a multipolar expansion of forces acting at the center of the defect. As in the Kanzaki approach, the addition of a point defect in a perfect crystal can be alternatively represented as a configuration of point forces acting on all affected, neighboring atoms. Consider a defect at the origin surrounded by N atoms (ν) with separation vectors $\mathbf{l}^{\nu}$. Following the formulations of Siems [10] and Teodosiu [11], the displacement field caused by a defect at the origin can expressed as

$$u_m(\mathbf{x}) = \sum_{\nu=1}^{N} G_{ms}(\mathbf{x}-\mathbf{l}^{\nu})P_s^{\nu}, \tag{1}$$

where $\mathbf{G}(\mathbf{x})$ is the elastic Green's tensor function of the material and $\mathbf{P}^{\nu}$ are the point forces acting on initial lattice atom locations $\mathbf{l}^{\nu}$. We note here that repeated indices imply summation. Expanding $\mathbf{G}(\mathbf{x}-\mathbf{l}^{\nu})$ in a Taylor's series about $\mathbf{x}$ gives

$$G_{ms}(\mathbf{x}-\mathbf{l}^{\nu}) = \sum_{k=0}^{\infty}\frac{(-1)^k}{k!}G_{ms,q_1\ldots q_k}(\mathbf{x})\mathbf{l}_{q_1}^{\nu}\ldots\mathbf{l}_{q_k}^{\nu} = G_{ms}(\mathbf{x}) - G_{ms,n}(\mathbf{x})\mathbf{l}_n^{\nu} + \frac{1}{2!}G_{ms,nq}(\mathbf{x})\mathbf{l}_n^{\nu}\mathbf{l}_q^{\nu} - \ldots.. \tag{2}$$

Plugging this Green's function expansion back into (1), the displacement field can be rewritten as

$$u_m(\mathbf{x}) = \sum_{k=0}^{\infty}\frac{(-1)^k}{k!}G_{ms,q_1\ldots q_k}(\mathbf{x})\mathbf{P}_{q_1\ldots q_k n}^{(k)} = G_{ms}(\mathbf{x})\mathbf{P}_s^{(0)} - G_{ms,n}(\mathbf{x})\mathbf{P}_{ns}^{(1)} + G_{ms,nq}(\mathbf{x})\mathbf{P}_{nqs}^{(2)} - \ldots, \tag{3}$$

where

$$\mathbf{P}_{q_1\ldots q_k s}^{(k)} = \sum_{\nu=1}^{N} l_{q_1}^{\nu}\ldots l_{q_k}^{\nu}\mathbf{P}_s^{\nu}, \qquad k = 1, 2, \ldots.., \infty \tag{4}$$

are called the multipole moments of kth order. It is important to note that the k=0 moment represents a sum of the applied force vectors over all atoms, which equals zero for equilibrium conditions to be satisfied. The k = 1, 2 and 3 moments are called the dipole, quadrupole, and octopole moments and can be expressed as

$$\begin{aligned}
\mathbf{P}^{(1)} &= \sum_{\nu=1}^{N}\mathbf{l}^{\nu}\mathbf{P}^{\nu} & P_{ns}^{(1)} &= \sum_{\nu=1}^{N} l_n^{\nu}P_s^{\nu} \\
\mathbf{P}^{(2)} &= \sum_{\nu=1}^{N}\mathbf{l}^{\nu}\mathbf{l}^{\nu}\mathbf{P}^{\nu} & P_{nqs}^{(2)} &= \sum_{\nu=1}^{N} l_n^{\nu}l_q^{\nu}P_s^{\nu} \\
\mathbf{P}^{(3)} &= \sum_{\nu=1}^{N}\mathbf{l}^{\nu}\mathbf{l}^{\nu}\mathbf{l}^{\nu}\mathbf{P}^{\nu} & P_{nqrs}^{(3)} &= \sum_{\nu=1}^{N} l_n^{\nu}l_q^{\nu}l_r^{\nu}P_s^{\nu}
\end{aligned} \tag{5}$$

The displacement equation (3) states that the elastic response of a defected material requires knowledge of the Green's function of the material and the values of the multipole moments of the defect. We point

out that this differs greatly from the Kanzaki approach in that all forces and higher order moments occur at the center of the defect, and not on lattice sites. To lowest order, the defect can be represented by the dipole tensor as is usually the case for defects of high symmetry (vacancies, interstitials, etc).

Solution Methodology

We have recently developed a hybrid method to compute the values for the multipolar moments of lattice defects using molecular statics (MS) calculations and continuum elasticity theory. Thus far, our focus has been on radiation induced defects in the bcc alpha-iron lattice. These defects include self-interstitial atoms (SIA), SIA clusters, helium point defects, and helium-vacancy clusters. Our method first requires an atomistic simulation of the defect in the host lattice to acquire the displacement field around the defect. For our molecular statics calculations we have chosen interatomic potentials well suited for simulation of these types of defects. For Fe-Fe, Fe-He, and He-He interactions we have chosen the well known Ackland [12], Juslin-Nordlund [13], and Lennard-Jones [14] interatomic potentials, respectively. In our atomistic calculations the defect was introduced in the center of the simulation box and a static relaxation (0 K) was implemented via conjugate gradient minimization to allow relaxation of the atoms. The lattice parameter used was 2.866 Angstroms. The supercell was a cube with an edge length of 18 lattice parameters (~52 Angstroms) and periodic boundary conditions were applied on all sides. This cell size was found to be large enough to contain the full extent of the lattice distortions produced, with the total number of host Fe atoms being 11664. After performing the MS calculations, the next step is to use the atomic displacement information to obtain a multipolar representation of the defect. Taking another look at equation (3), we can alternatively view this equation as a matrix-vector multiplication of the form

$$\{u\} = [G]\{P\}. \tag{6}$$

In this light, {u} is a 3N by 1 column vector containing the MS displacement vector components of N chosen neighboring atoms and can be expressed as $\{u\} = \{\{u_1, u_2, u_3\}_1 \{u_1, u_2, u_3\}_2 .... \{u_1, u_2, u_3\}_N\}^T$. The column vector {P} represents the values of the chosen multipolar moments used to describe the defect. It has size $N^{(k)}$ by 1, where $N^{(k)}$ equals the total number of multipolar values chosen to be solved for. For example, if the dipole moment is sufficient to represent the defect, then $N^{(k)} = 9$. This vector can be expressed as $\{P\} = \{\{P_{11}, P_{12}, ... P_{33}\}^{(1)} ... \{P_{1...1}, P_{1...2}, ... P_{3...3}\}^{(k)}\}^T$. The matrix [G] represents the corresponding elastic Green's function derivatives evaluated at the desired field point. This matrix has size 3N by $N^{(k)}$. We have found that the use of the isotropic elastic Green's function provides adequate response of the material as compared to our MS calculations. This response function is well known and provides a tractable closed-form solution simplifying the necessary calculations. It can be expressed as

$$G_{ms}(\vec{x}) = \frac{1}{8\pi\mu(\lambda + 2\mu)} \left[(\lambda + 3\mu)\frac{\delta_{ms}}{r} + (\lambda + \mu)\frac{x_m x_s}{r^3} \right], \tag{7}$$

where the Lamé's constants λ and μ define the material, and r = $\sqrt{x_i x_i}$. The multipole (k) value also implies the order of derivative of the Green's function necessary for the calculations. We note these derivatives fall off as $O(r^{-(k+1)})$. While the displacement field contributions decay rapidly for k>1, and the dipole moment dominates at longer distances, we have typically found the inclusion of up to the octopole tensor, to be necessary to accurately match the lattice displacements near the defect. With the values of {u} and [G] known from MS calculations and elasticity theory, respectively, equation (6) can be posed as a least squares optimization problem which can then be solved to obtain the multipole moment values {P}. This step has a significant benefit since displacements beyond the first few shells may also be used to extract information about the defect.

The lifetime and fate of point defects operating in radiation damaged environments are governed by the many elastic interactions they may have with any number of other defects within the host material. These interactions affect the stability and migration tendencies of defects and have been a topic of great concern within the nuclear materials community for some time. Thus, it is of most importance to have a detailed, quantitative understanding of these interactions. Consider again a point defect at **x** modeled as

a configuration of point forces $\mathbf{P}^{\nu}$ acting on neighboring atoms ν, this time placed within an existing displacement field **u**. It is clear that the resulting interaction energy can be expressed as

$$E_{int} = -\sum_{\nu=1}^{N} \mathbf{P}^{\nu} \cdot \mathbf{u}(\mathbf{x} + \mathbf{l}^{\nu}). \tag{8}$$

Now expanding $\mathbf{u}(\mathbf{x}+\mathbf{l}^{\nu})$ in a Taylor's series about **x** we have

$$u_m(\mathbf{x} + \mathbf{l}^{\nu}) = u_m(\mathbf{x}) + u_{m,i}(\mathbf{x}) l_i^{\nu} + \frac{1}{2!} u_{m,ij}(\mathbf{x}) l_i^{\nu} l_j^{\nu} + \frac{1}{3!} u_{m,ijk}(\mathbf{x}) l_i^{\nu} l_j^{\nu} l_k^{\nu} + \ldots \tag{9}$$

Introducing this expression back into (8), allows the interaction energy to be expressed in terms of the multipolar moments as

$$E_{int} = -\sum_{n=1}^{\infty} \frac{1}{n!} u_{m,q_1 \ldots q_n}(\mathbf{x}) \mathbf{P}^{(n)}_{q_1 \ldots q_n m} = -\mathbf{P}^{(1)}_{im} u_{m,i}(\mathbf{x}) - \frac{1}{2!} \mathbf{P}^{(2)}_{ijm} u_{m,ij}(\mathbf{x}) - \frac{1}{3!} \mathbf{P}^{(3)}_{ijkm} u_{m,ijk}(\mathbf{x}) - \ldots \tag{10}$$

Applications

The focus of our research has been primarily on radiation induced defects in the bcc α-iron lattice. In this section we will highlight some representative results obtained for a small selection of defects that have been modeled.

I. Fe SIA <110> dumbbell

Self interstitial atoms (SIA) are generated in significant quantities in fission, and to a larger extent, fusion reactors. They are produced in the wake of displacement cascades caused by incoming fluxes of high energy neutrons. Studies of the energetics and mechanisms of migration for these point defects have been a topic of interest for many years. Single SIAs in α-iron take the form of a split dumbbell configuration. In the past, experimental studies [15], as well as ab-initio calculations [16,17], have concluded the ground state configuration to be the <110> dumbbell. In our MS calculations, we have found the formation energy to be 3.35 eV, which is in agreement with values reported previously by Terentyev, *et al* [18], but lower than those predicted by DFT. Implementing our hybrid method for multipolar representation of this defect, we have calculated the multipolar moments up to the octopole tensor ($\mathbf{P}^{(3)}$). Calculated values for the dipole tensor are given in table 1. In figure 1 we have plotted the displacements versus distance from the defect center. The plots on the left and right show the radial and Cartesian components, of the displacements, respectively. The circles in these plots are those obtained from MS calculations, while the points represent the calculated displacements using the multipolar representation via equation (3).

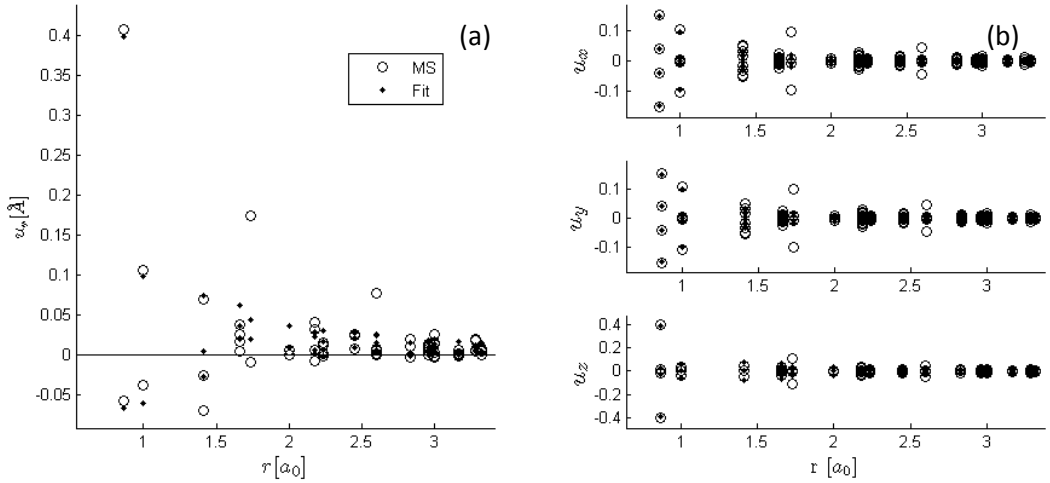

Figure 1. Displacement vs. radial distance plots for [110] Fe SIA. (a) radial (b) Cartesian components.

We see very good agreement in the displacements predicted by the multipolar representation. First, it is important to note the complexity of the lattice response to this defect. In the first shell alone we see the very large expansion of the four atoms lying on the (110) plane with a contraction of the remaining four atoms. This immediately suggests any attempt to model this defect as an inclusion or center of dilatation would be in vain. In fact we have found that without the inclusion of the octopole moment, the dipole tensor alone struggles to replicate these phenomena. The largest contribution to elastic energy is contained within the first few shells around the defect, and we see very good agreement in this vicinity. To obtain an overall quantity to compare the accuracy of this new multipolar representation of the defect compared to the MS calculations, we have chosen to compare the predicted formation energy of both representations. To do this, we apply the multipole displacements to a perfect bcc Fe lattice and hold these new positions fixed. Next we evaluate the energy of this system using the Fe interatomic potential. This allows direct comparison of the formation energies. We find the multipolar representation to give a formation energy of 4.02 eV giving a percent difference of roughly 20% with the MS value. This over-prediction stems from the inherent inability of continuum elasticity to account for the intricate atomic interactions that occur within the discrete atomic lattice. We also note this percent difference lies within the variation of several Fe interatomic potentials [23].

We have recently studied the effect of deformation on the formation energy of SIAs in α-iron [19]. This problem is important in severe radiation conditions where the lattice undergoes deformations under applied loads. Ab-initio calculations were made for various strain loadings of volumetric and uniaxial type. These calculations were then compared to results from obtained using MS calculations with the above mentioned interatomic potential, and also with the multipolar representation of the defect using continuum elasticity (CE) formulations. The formation energy of a defect in a strained environment can be computed as

$$E^f = E_0^f + E_{int} \tag{11}$$

where E_0^f represents the equilibrium formation energy of the defect and E_{int} is the elastic interaction of the defect with the strain field. As a reference, we have taken E_0^f to be that calculated by MS. In a homogeneous strain field, we see from equation (10) the interaction term can be computed as

$$E_{int} = -P_{ij}^{(1)} \varepsilon_{ij} \,. \tag{12}$$

This equation implies that under constant strain, only the dipole moment contributes to the interaction energy. In the case of defect interactions with varying strain fields (dislocations, grain boundaries, other point defects), this will not be the case, and the higher order moments will contribute to the interactions. Results for formation energies of the [110] SIA under both strain modes can be found in figure 2. For volumetric strains, the applied strain tensor can be expressed as $\varepsilon_{ij}=\varepsilon_v/3\ \delta_{ij}$, and for uniaxial strains the only nonzero component was ε_{33}.

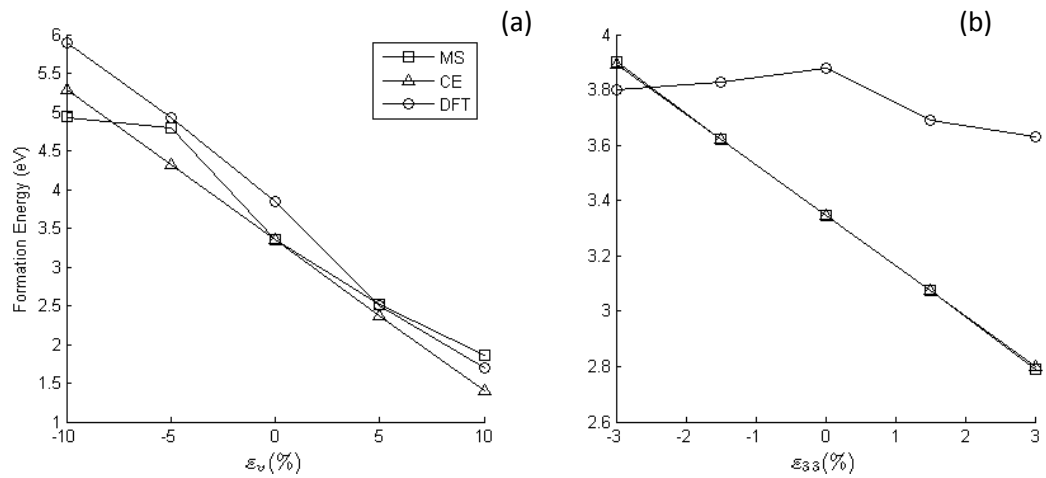

Figure 2. Formation energy vs. applied external strain for [110] Fe SIA. (a) Volumetric (b) Uniaxial.

In the volumetric strain studies we found very good agreement in the energetic trends. The linear behavior of energetic favorability of defect formation under lattice expansion is predicted by the continuum approach and verified by the MS and ab initio calculations. The discrepancies in the values can be attributed to several causes. Above all, the formation energy of a defect will contain contributions of both elastic and electronic interaction with the host lattice. The MS calculations do not account for these electronic interactions though they do contain information about the lattice. The continuum elasticity solutions contain neither energetic contributions from the lattice structure nor the electronic interactions and thus predict lower formation energies compared to the ab-initio calculations. Under uniaxial strain we see near identical prediction of the formation energy in the MS and continuum calculations. However the predicted trends in both defects are not observed in the ab-initio results. This suggests highly influential electronic reconfigurations are at play in uniaxial deformations.

II. Helium point defects

Extrinsic radiation induced defects are well known to contribute to the mechanisms of damage accumulation and evolution in irradiated materials. Substantial quantities of helium atoms are generated within the α-iron lattice by (n,α) transmutation reactions. Helium is highly insoluble in iron and thus interstitials rapidly migrate with an energy barrier less than 20% than that of Fe interstitials [20]. We have undergone calculations of the multipole moments for helium in both octahedral and substitutional configurations. The results for these calculations are found in table 1. Figure 3 (a) shows the radial displacement versus distance for the octahedral interstitial.

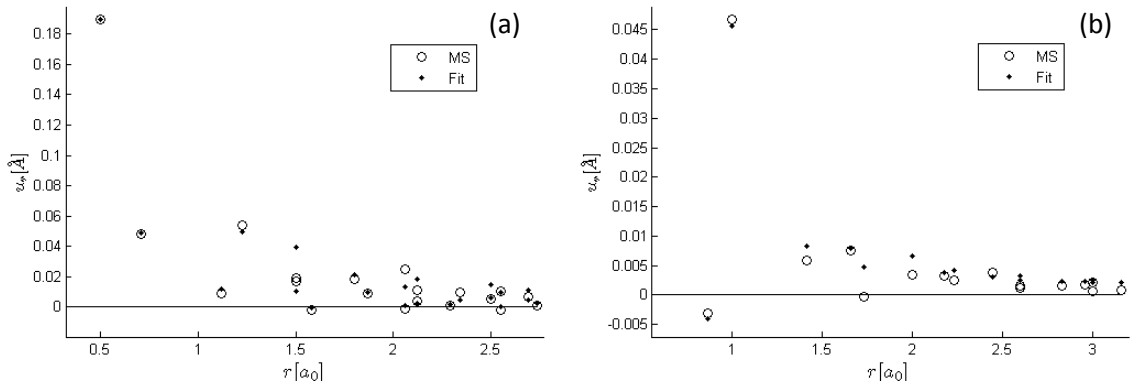

Figure 3. Radial displacement vs. distance plots for helium point defects in α-Fe. (a) Octahedral (b) Substitutional.

We see excellent agreement in the first four atomic shells, with an over-prediction in the slightly anisotropic fifth shell, but good decay agreement in the shells that follow. We found it necessary to implement the octopole moment in order to get good matching for the displacements in the third and fourth shell. Comparing the formation energies between MS and the multipole representation, we found the percent difference to be only 0.89% between the continuum value (4.49 eV) and the MS value (4.45 eV).

The displacement field generated by the substitutional helium is somewhat more complex (see figure 3 (b)). In our MS calculations we find a 0.307 pm radial contraction of the 8 nearest neighbors, contrasted by a 4.67 pm expansion of the 6 second nearest neighbors. This behavior is not well suited for classical elasticity and we find the use of the octopole tensor as the only way to account for the discontinuity. Our calculations give a percent difference of 33% and 2.3% in the radial displacements of the first two shells, respectively, and we find the octopole tensor to assume only six non-zero components. We note the large percent difference in the first shell is due to the very small contraction, and does not influence the defect energy to the extent the second shell does.

Table 1. Computed dipole tensor values (in eV) for selected defects in α-Fe. (*P_{12}/P_{21} given for HeV cluster)

	P_{11}	P_{22}	P_{33}	P_{12}	P_{23}	P_{13}
Octahedral Helium	5.37	5.37	8.73	0.00	0.00	0.00
Substitutional Helium	3.51	3.51	3.51	0.00	0.00	0.00
[110] Fe SIA Dumbbell	20.02	20.02	18.22	-9.107	0.00	0.00
He12V4 Cluster	64.65	71.91	72.84	0.606/-0.095*	0.00	0.00

III. Helium vacancy clusters

The rapid diffusion of helium within the host lattice is halted as these solute atoms meet their fate at system sinks such as dislocations, grain boundaries, and vacancy voids. Helium has long been known to stabilize voids against their otherwise collapse by vacancy emission [21], and lead to swelling in the material. The stability and migration energetics of helium-vacancy clusters (He_nV_m) have been studied in the past using atomistic simulations [20,21]. We have found our hybrid multipole method to accurately mimic the displacements seen in MS calculations of these defects. We describe here the results of our calculations for a $He_{12}V_4$ cluster. This defect was found to produce a highly anisotropic displacement field in the lattice and illustrates the point that when the higher order multipolar moments are included, then isotropic elastic Green's functions are capable of predicting these non-uniformities. The defect was created by adding 12 atoms into 4 vacancies in a random fashion. Then dynamics were run at 100 K for 1 ns allowing the cluster reach a more energetically favorable configuration. Lastly the defect and lattice were allowed to relax at 0 K. We do not suggest here that this particular final configuration is the ground state of the defect. Figure 4 shows the displacement field of the defect. 14 nonzero components

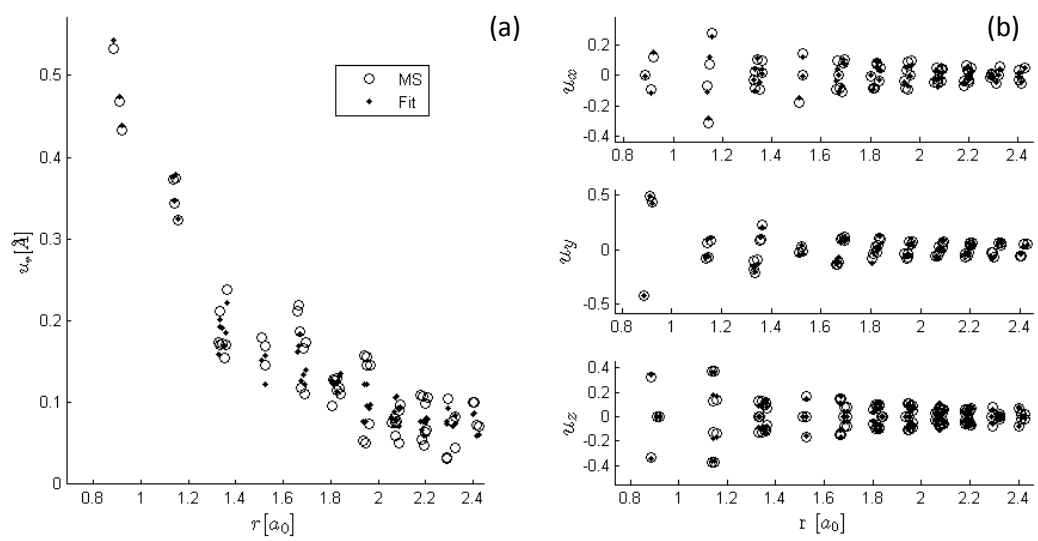

Figure 4. Displacement vs. radial distance plots for a $He_{12}V_4$ cluster in α-Fe. (a) radial (b) Cartesian components.

We chose to define the center of the defect to be the center of mass of the helium atoms within the cluster in the final configuration which explains the minor radial variations in the shell distances. We note the very close agreement in the atomic displacements within about 1.7 lattice parameters of the defect center. In this region the discrete lattice effects will be maximum, however we see isotropic elasticity is capable of reproducing this foreign nature. Furthermore, the fitting scheme was generated using the MS displacements of 40 neighboring atoms which includes all atoms within this region. The elasticity-predicted decay beyond this point is seen to match well with the MS calculations. We note the asymmetry of the dipole tensor for this defect as seen in table 1. It is found that $P_{12} \neq P_{21}$ which suggests the defect is not without moment.

Elastic Interactions of Defects

With the multipolar values known for various defects, equation (10) may be implemented to calculate interaction energy fields between defects. Plotted in figure 5 are the interaction energy contours of (a) an octahedral helium interstitial and (b) an Fe [110] SIA atom, with a $He_{12}V_4$ cluster residing at the center.

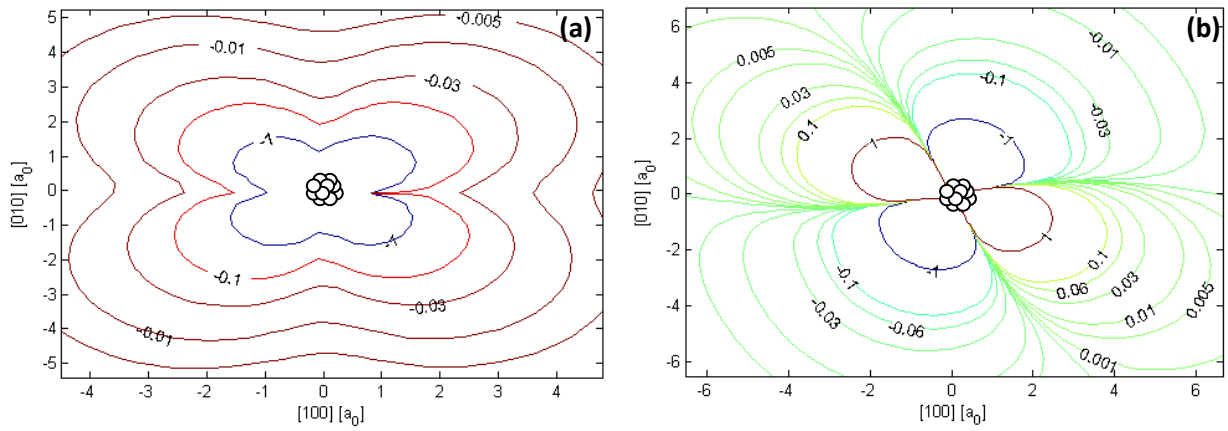

Figure 5. Iso-interaction energy contours (in eV) of (a) He octahedral (b) [110] Fe SIA dumbbell, with $He_{12}V_4$ cluster at the origin in α-Fe.

The interaction energy contours in (a) show attraction between the defects at all positions on the (100) plane. This elastic attraction which leads to cluster growth is well known to exist between interstitial helium atoms and HeV clusters, and is confirmed by our elasticity calculations. The iron SIA on the other hand shows four distinct regions around the HeV cluster. Two regions that indicate a repulsive interaction, and two that show attraction. We propose that for a sufficiently strong repulsive interaction near the cluster, one of two phenomena may occur. The SIA will either rotate its orientation to a more energetically favorable configuration, or migrate to one of the attractive regions. Its choice will obviously depend on the energy barriers involved in those processes. In these plots we note that not all positions will be available to the point defects due to the presence of the host lattice, however we find the trends and energy scales very useful.

We have also conducted calculations between extended- and point defects. Using the edge dislocation model given in Hirth and Lothe [22] for an infinite isotropic elastic solid, we have obtained interaction energy contours for the multipolar defects. These calculations are meant only to be approximations, especially near the dislocation core where the singularity causes divergence in the energy. Plotted in figure 6 are the interaction energy contours of (a) an octahedral helium interstitial and (b) an Fe [110] SIA atom, with an $a_0/2[111]\{110\}$ edge dislocation in iron.

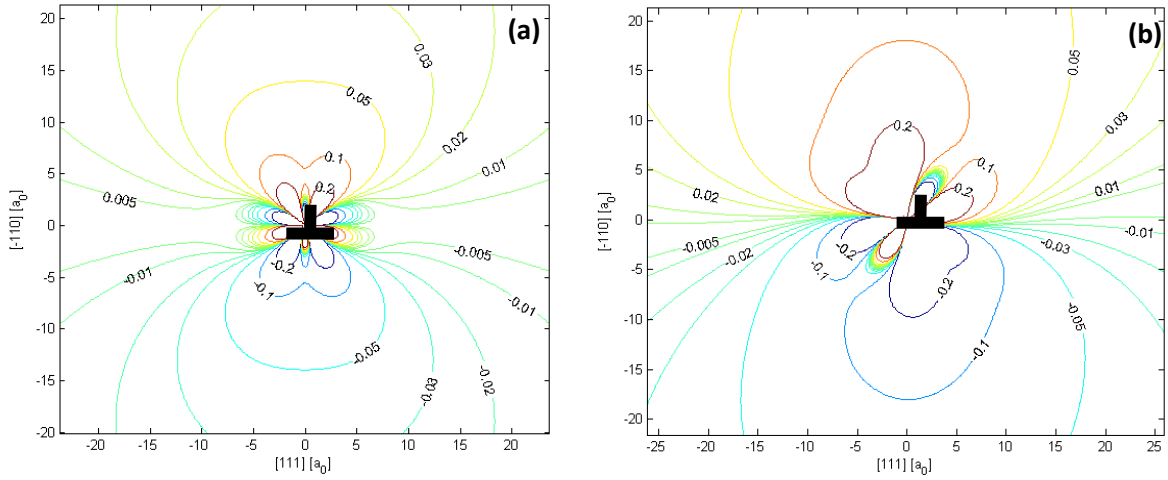

Figure 6. Iso-interaction energy contours (in eV) of (a) He octahedral (b) [110] Fe SIA dumbbell, with an $a_0/2[111]\{110\}$ edge dislocation in α-Fe.

In both plots of figure 6 we see the tendency for the interstitials to be drawn to the dislocation core while on the tensile side of the dislocation (repulsion is seen on the compressive side). We also see some higher order effects in the contours of both cases within roughly 5 a_0 of the dislocation. These effects fade with distance as the dipole tensor term in equation (10) dominates the interaction. The strength and extent of interaction of the Fe interstitial with the dislocation is found to be roughly 2.5 times greater than that of the helium interstitial.

Conclusion

In this study, a hybrid method has been developed to couple the results of molecular statics calculations with classical isotropic elasticity theory to extract a continuum representation of various defects through the use of force multipoles. These calculations have provided a means to account for the changes in defect energetics due to local strain environment effects. The isotropic elastic Green's function is found to provide material response very consistent with atomistic simulations when higher order moments describing the defect are implemented. We have found the use of the octopole tensor in many cases is necessary, and is able to capture anisotropies in the displacement field as well as discrete lattice irregularities, both of which are foreign phenomena within isotropic elasticity theory.

We have also performed calculations of the interaction energies between multipolar defects and intrinsic extended defects in iron. Our solutions have thus far provided approximations for the energetics and general trends in the affinity of defects to show attraction or repulsion to other defects. We are currently developing hybrid methods to model dislocations and grain boundaries, to use in these calculations for increased accuracy. The method we describe and its outcomes will allow for more accurate models of defect diffusion and interaction within the radiation damage environment, where long- and short-range elastic interactions govern the accumulation and evolution of defects in the material.

References

[1] L.K. Mansur, Journal of Nuclear Materials 216 (1994), 97.
[2] B.N. Singh, H. Trinkaus, A.J.E. Foreman, Journal of Nuclear Materials 249 (1997), 103.
[3] C. Domain, C.S. Becquart, L. Malerba, Journal of Nuclear Materials 335 (2004), 121.
[4] K. Morishita, R. Sugano, Nuclear Instruments and Methods in Physics Research B 255 (2007), 52.
[5] B.D. Wirth, E.M. Bringa, Physica Scripta 108 (2004), 80.
[6] H. Kanzaki, Journal of Physics and Chemistry of Solids 2 (1957), 24.
[7] R. Bullough and J. Hardy , Philosophical Magazine 17 (1968), 833.
[8] C.S. Hartley and R. Bullough, Journal of Applied Physics 48 (1977), 4557.
[9] J.D. Eshelby, Journal of Applied Physics 25 (1954), 255.
[10] R. Siems, Physica Status Solidi, 30 (1968), 645.
[11] C. Teodosiu, Springer, Berlin, Heidelberg, New York, (1982).
[12] G.J. Ackland, M.I. Mendelev, D.J. Srolovitz, S. Han, and A.V. Barashev, Journal of Physics: Condensed Matter 16 (2004), S2629.
[13] N. Juslin and K. Nordlund, Journal of Nuclear Materials 382 (2008), 143.
[14] J.E. Lennard-Jones, Proceedings of the Royal Society A 106 (1924), 463.
[15] P. Ehrhart, K.H. Robrock, and H.R. Schober, Elsevier-Amsterdam (1986), 63.
[16] C. Domain and C.S. Becquart, Physical Review B 65 (2002), 024103.
[17] C.C. Fu, F. Willaime, and P. Ordejon, Physical Review Letters 92 (2004), 175503.
[18] D.A. Terentyev, L. Malerba, and M. Hou, Physical Review B 75 (2007), 104108.
[19] Z.Z. Chen, N. Kioussis, N.M. Ghoniem, and D. Seif, (submitted for publication).
[20] M.J. Caturla, C.J. Ortiz, C.C. Fu, Comptes Rendus Physique 9 (2008), 401.
[21] K. Morishita, R. Sugano, B.D. Wirth, T. Diaz de la Rubia, Nuclear Instruments and Methods in Physics Research B 202 (2003), 76.
[22] J.P. Hirth and J. Lothe, John Wiley & Sons, (1982).
[23] B.J. Lee and M.I. Baskes, Physical Review B 62 (2000), 8564.